Electromagnetic corrections and the $\pi^+e^+e^-$ invariant-mass distribution in $K^+\to\pi^+e^+e^-$

M. Soldate
Center for Theoretical Physics, Yale University, 217 Prospect Street, New Haven, Connecticut 06511
(Received 13 August 1991; revised manuscript received 23 December 1991)

The dominant first-order electromagnetic corrections to the $\pi^+e^+e^-$ invariant-mass distribution of the rare decay $K^+\to\pi^+e^+e^-$ are analyzed.

PACS number(s): 13.40.Ks, 13.20.Eb

I. INTRODUCTION

Electromagnetic radiative corrections in K decays with final-state electrons or positrons can be sizable in general because the electron mass is small compared with the K mass. A light charged lepton would undergo effectively large accelerations in its creation and so should radiate significantly. In practice, then, radiative corrections contain large logarithms of a ratio of scales roughly proportional to m_K/m_e, which act to suppress stringently nonradiative processes.

Recently, the rare decay $K^+\to\pi^+e^+e^-$ has been studied experimentally with considerable accuracy [1,2]. This report provides an examination of the effect of electromagnetic radiative correlations on the $\pi^+e^+e^-$ (πee) invariant-mass distribution for this process. In the experiment referred to above, the momenta of only charged tracks are measured. In particular, the momentum carried off by a photon goes undetected. Under these circumstances the πee invariant mass need not be the K mass, but an approximate K mass can be inferred from the πee invariant-mass distribution given adequate theoretical input. Here the πee invariant-mass distribution is calculated in lowest nontrivial order in the simplest appropriate approximation scheme as explained below. Previous treatments of electromagnetic radiative corrections in π and K decays include [3].

II. CALCULATION

The object is to calculate approximately the πee invariant-mass ($m_{\pi ee}$) distribution in $K^+\to\pi^+e^+e^-$ to order α in electromagnetic corrections. One-photon emission is allowed; the photon is assumed to go undetected. The πee invariant-mass square is $m^2_{\pi ee}=(p_\pi+r_1+r_2)^2$ in the notation of Figs. 1(a) and 1(b).

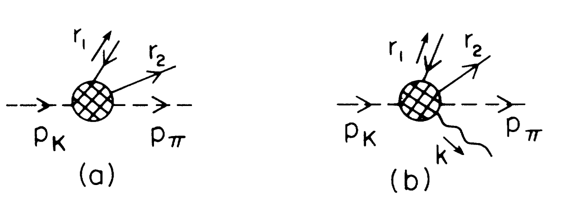

FIG. 1. Labeling of momenta in the reactions (a) $K^+\to\pi^+e^+e^-$ and (b) $K^+\to\pi^+e^+e^-\gamma$.

Some features of the experiment allow for simplifying approximations. The most important one is that the e^+e^- invariant mass m_{ee} is required to be greater than m_{π^0}. This is necessary to avoid the background from $K^+\to\pi^+\pi^0$ followed by $\pi^0\to e^+e^-\gamma$, where the γ is undetected. Then, for example, the ratio m_e/m_{ee} can be assumed to be small. The largest radiative corrections are those which contain logarithms of m_e divided by a scale of order m_π or m_K. This paper is concerned exclusively with such terms.

The dominant contribution to the process with or without radiative corrections arises from virtual-photon rather than Z exchange, as illustrated in Fig. 2. The graphs of the type Fig. 1(a), which are discussed here in detail, are illustrated in Fig. 3, while those of type Fig. 1(b) are illustrated in Fig. 4. These form gauge-invariant sets and contain the dominant large logarithms involving the electron mass. Note in this regard that in the soft-photon approximation the interference terms between photon emission from a lepton and from a hadron cancel when evaluating the $m_{\pi ee}$ distribution. Another class of graphs of type Fig. 1(a) which is relevant is illustrated in Fig. 5. In the Appendix the sum of such graphs is argued to contain at most single logarithms of the electron mass, subdominant to the leading double logarithms arising from the graphs of Figs. 3 and 4. The coefficient of the single logarithm from the class of graphs in Fig. 5 appears to depend on hadronic quantities presently incalculable and unavailable from the present experiment. Therefore the graphs in Fig. 5 introduce an element of uncertainty which will be specified in the concluding remarks.

The amplitude without radiative corrections, illustrated in Fig. 2, is

$$\mathcal{M}_0(K\to\pi ee)=F((r_1+r_2)^2)p_K^\lambda\bar{u}(r_2)\gamma_\lambda v(r_1)\ , \qquad (1)$$

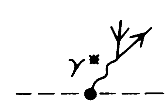

FIG. 2. Virtual-photon contribution dominates over the virtual-Z contribution.

(a) (b)

FIG. 3. Virtual corrections analyzed in detail in this report.

(a) (b)

FIG. 4. Real-emission corrections analyzed in this report.

where F includes a form factor, the photon propagator, and constants. Only radiative corrections corresponding to Figs. 3 and 4 depend in general on no more hadronic information than is contained in F. The presence of the form factor precludes a fully analytic treatment. The results will be presented in a form suitable for Monte Carlo evaluation. For example, the uncorrected partial width Γ_0 is

$$\Gamma_0=\frac{1}{2m_K}\int\frac{d^3\mathbf{p}_\pi}{(2\pi)^3 2\epsilon_\pi}\int d^4q\;\theta[q^0-(\mathbf{p}_\pi^2+4m_e^2)^{1/2}](2\pi)^4\delta^4(p_K-p_\pi-q)$$
$$\times\frac{1}{8(2\pi)^6}(1-4m_e^2/q^2)^{1/2}\int d^2\Omega_{\hat{\mathbf{R}}_1}\sum_{\text{spins}}|\mathcal{M}_0(K\to\pi ee)|^2\;. \tag{2}$$

Here $\hat{\mathbf{R}}_1$ is the three-momentum direction of the positron in the e^+e^- center-of-mass frame (for each four vector q^μ). The θ function is appropriate as written for p_π^μ and q^μ given in the K rest frame. Of course, without radiation, $m_{\pi ee}=m_K$. Terms of order m_e^2/q^2 have been retained for the moment.

The radiative corrections are of either virtual (Fig. 3) or real emission (Fig. 4) in type. They have two effects on the $m_{\pi ee}$ distribution. First, the real-emission corrections generate a tail for the distribution so that it is not a δ-function distribution, as it would be otherwise (ignoring the intrinsic width of the K). Second, the virtual- and real-emission effects combine to suppress the quantity $\int_{(m_K-\Delta_m)^2}^{m_K^2}dm_{\pi ee}^2(d\Gamma/dm_{\pi ee}^2)$, essentially the magnitude of the peak. This quantity will be referred to as the contribution of the first bin. The two sorts of radiative corrections, when combined in the first bin, cancel their individual infrared divergences. The bin size Δm acts as the resolution in $m_{\pi ee}$.

Provided that $m_{\pi ee}$ is not too different from m_K, the soft-photon approximation can be used. More quantitative statements will be made later. The soft-photon approximation will be used below. Infrared divergences will be regulated dimensionally [4,5], and the soft-photon approximation will be made following the approach and notation of [5] and references therein.

The $m_{\pi ee}^2$ distribution for $m_{\pi ee}\neq m_K$ can be written as

$$\frac{d\Gamma}{dm_{\pi ee}^2}=\frac{1}{2m_K}\int\frac{d^3\mathbf{p}_\pi}{(2\pi)^3 2\epsilon_\pi}\int d^4q\;\theta[q^0-(\mathbf{p}_\pi^2+4m_e^2)^{1/2}](2\pi)^4\delta^4(p_K-p_\pi-q)\frac{d\gamma}{dm_{\pi ee}^2}\;, \tag{3}$$

where

$$\frac{d\gamma}{dm_{\pi ee}^2}=\int\frac{d^3\mathbf{r}_1}{(2\pi)^3 2\epsilon_1}\frac{d^3\mathbf{r}_2}{(2\pi)^3 2\epsilon_2}\frac{d^{n-1}\mathbf{K}}{(2\pi)^{n-1}2|\mathbf{K}|}\delta^4(q-r_1-r_2-k)\sum_{\text{spins}}|\mathcal{M}(K\to\pi ee\gamma)|^2\delta(m_{\pi ee}^2-(p_\pi+r_1+r_2)^2)\;. \tag{4}$$

Here the final-state photon phase-space factor $d^3\mathbf{k}/(2\pi)^3 2|\mathbf{k}|$ has been written somewhat symbolically in its dimensionally regulated form. The introduction of the auxiliary momentum q^μ is convenient for the graphs of Fig. 4. $d\gamma/dm_{\pi ee}^2$, a Lorentz invariant, is most easily evaluated in the $e^+e^-\gamma$ center-of-mass frame, for given q^μ. In this frame, $q^\mu=(Q,\mathbf{0})$, $p_\pi^\mu=(E_\pi,\mathbf{P}_\pi)$, and $r_j^\mu=(E_j,\mathbf{R}_j)$. In the soft-photon approximation and also dropping terms of order m_e^2/Q^2,

$$\frac{d\gamma}{dm_{\pi ee}^2}\to\int d^2\Omega_{\hat{\mathbf{R}}_1}\sum_{\text{spins}}|\mathcal{M}_0(K\to\pi ee)|^2\frac{e^2}{2^n(2\pi)^{n+5}}(m_K^2-m_{\pi ee}^2)^{n-5}$$
$$\times\int d^{n-2}\Omega_{\hat{\mathbf{K}}}\left[\frac{1}{Q+E_\pi-\hat{\mathbf{K}}\cdot\mathbf{P}_\pi}\right]^{n-4}\left[\frac{Q^2}{(E_1-\mathbf{R}_1\cdot\hat{\mathbf{K}})(E_1+\mathbf{R}_1\cdot\hat{\mathbf{K}})}\right.$$
$$\left.-m_e^2\left[\frac{1}{(E_1-\mathbf{R}_1\cdot\hat{\mathbf{K}})^2}+\frac{1}{(E_1+\mathbf{R}_1\cdot\hat{\mathbf{K}})^2}\right]\right]\;, \tag{5}$$

where $E_1\simeq Q/2$.

The validity of the soft-photon approximation can be estimated as follows. The e^+e^- pair is produced over a region roughly of size $1/(q^2)^{1/2}$. For $|\mathbf{K}|$ smaller than $(q^2)^{1/2}$, the details of the leptonic current trajectories are weakly probed, and the soft-photon approximation should be reasonable [6]. In making more specific estimates, the slightly more conservative range $|\mathbf{K}| \lesssim E_j$ (i.e., E_1 or E_2) will be used. For $|\mathbf{K}| \gtrsim m_\pi/2$ and $m_{ee} \simeq m_\pi$, then, the soft-photon approximation will be inaccurate. In obtaining the form Eq. (5), $|\mathbf{K}|$ has been fixed to be

$$|\mathbf{K}| = \frac{m_K^2 - m_{\pi ee}^2}{2(Q + E_\pi - \hat{\mathbf{K}}\cdot\mathbf{P}_\pi)} . \tag{6}$$

The minimum value of $m_K - m_{\pi ee}$ consistent with $|\mathbf{K}| \simeq m_\pi/2$ and $m_{ee} \simeq m_\pi$ is $m_K - m_{\pi ee} \simeq 3m_\pi^2/4m_K \simeq 30$ MeV. At this value of $m_K - m_{\pi ee}$, values of $|\mathbf{K}|$ ranging to roughly 10 times smaller are also relevant. Therefore the soft-photon approximation will just begin to breakdown at $m_K - m_{\pi ee} \simeq 30$ MeV. The experiment [1,2] is concerned primarily with $m_K - m_{\pi ee} \lesssim 30$ MeV, and so the soft-photon approximation is appropriate. This is the second simplification allowed by the particulars of the experiment in question.

Continuing with the evaluation of $d\gamma/dm_{\pi ee}^2$, the integral $d^{n-2}\Omega_{\hat{\mathbf{K}}}$ can be done in the peaking approximation. For $f(\hat{\mathbf{K}})$ slowly varying close to $\hat{\mathbf{K}} = \hat{\mathbf{R}}_1$ or $\hat{\mathbf{R}}_2 \simeq -\hat{\mathbf{R}}_1$,

$$\begin{aligned}\int d^{n-2}\Omega_{\hat{\mathbf{K}}} &\left[\frac{Q^2}{(E_1 - \mathbf{R}_1\cdot\hat{\mathbf{K}})(E_1 + \mathbf{R}_1\cdot\hat{\mathbf{K}})} - m_e^2\left[\frac{1}{(E_1 - \mathbf{R}_1\cdot\hat{\mathbf{K}})^2} + \frac{1}{(E_1 + \mathbf{R}_1\cdot\hat{\mathbf{K}})^2}\right]\right] f(\hat{\mathbf{K}}) \\ &\simeq 2\pi \frac{\pi^{n/2-2}}{\Gamma(n/2-1)}\left\{2\ln\left[\frac{Q^2}{m_e^2}\right] + (n-4)\left[-\frac{1}{2}\ln^2\left[\frac{Q^2}{m_e^2}\right] + (2\ln 2 + 1)\ln\left[\frac{Q^2}{m_e^2}\right]\right]\right\}[f(\hat{\mathbf{K}} = \hat{\mathbf{R}}_1) + f(\hat{\mathbf{K}} = -\hat{\mathbf{R}}_1)] . \end{aligned} \tag{7}$$

The terms proportional to $n-4$ must be retained in the calculation of the contribution of the first bin because the integral over $m_{\pi ee}^2$ there yields an infrared pole term proportional to $1/(n-4)$. Evaluation of the $O(1)$ terms requires a calculation beyond the peaking approximation (for a related example, see [7]).

In the soft-photon approximation and dropping terms of $O(m_e^2/Q^2)$, the graphs of Fig. 4 give

$$\begin{aligned}\frac{d\Gamma_{(4)}}{dm_{\pi ee}^2} \simeq \frac{1}{2m_K}\int \frac{d^3\mathbf{p}_\pi}{(2\pi)^3 2\epsilon_\pi}\int d^4q\, \theta[q^0 - (\mathbf{p}_\pi^2)^{1/2}]\theta(q^2 - q_{\text{cut}}^2)(2\pi)^4\delta^4(p_K - p_\pi - q)\frac{1}{8(2\pi)^6} \\ \times \int d^2\Omega_{\hat{\mathbf{R}}_1}\sum_{\text{spins}}|\mathcal{M}_0(K\to\pi ee)|^2 \frac{\alpha}{\pi}\frac{2}{m_K^2 - m_{\pi ee}^2}\left[\ln\left[\frac{Q^2}{m_e^2}\right] + O(1)\right] ,\end{aligned} \tag{8}$$

outside of the first bin, and

$$\begin{aligned}\int_{(m_K-\Delta m)^2}^{m_K^2} & dm_{\pi ee}^2 \frac{d\Gamma_{(4)}}{dm_{\pi ee}^2} \\ &\simeq \frac{1}{2m_K}\int \frac{d^3\mathbf{p}_\pi}{(2\pi)^3 2\epsilon_\pi}\int d^4q\, \theta[q^0 - (\mathbf{p}_\pi^2)^{1/2}]\theta(q^2 - q_{\text{cut}}^2)(2\pi)^4\delta^4(p_K - p_\pi - q)\frac{1}{8(2\pi)^6} \\ &\quad\times \int d^2\Omega_{\hat{\mathbf{R}}_1}\sum_{\text{spins}}|\mathcal{M}_0(K\to\pi ee)|^2 \frac{\alpha}{\pi}\left\{\ln\left[\frac{Q^2}{m_e^2}\right]\left[\frac{2}{n-4} + \gamma_E - \ln(16\pi) \right.\right. \\ &\qquad\left. + \ln\left[\frac{4m_K^2(\Delta m)^2}{(Q+E_\pi)^2 - (\hat{\mathbf{R}}_1\cdot\mathbf{P}_\pi)^2}\right]\right] \\ &\qquad\left. - \frac{1}{2}\ln^2\left[\frac{Q^2}{m_e^2}\right] + (2\ln 2 + 1)\ln\left[\frac{Q^2}{m_e^2}\right] + O(1)\right\} .\end{aligned} \tag{9}$$

The quantity q_{cut}^2 is the lower cutoff on the e^+e^- invariant mass, of order m_π^2.

The virtual corrections of Fig. 3 are also required to complete the calculation of the contribution of the first bin only. The asymptotic behavior of the vertex function (including the effect of wave-function renormalization) and vacuum polarization (including charge-renormalization effects) are well known [7–9]. Including on-shell wave-function renormalization, the ultraviolet-finite vertex function at large timelike q^2 is (in the notation of [10])

$$\Gamma_c^\mu(p',p) = F_1(q^2,m_e^2)\bar{u}(p')\gamma^\mu v(p) + \frac{F_2(q^2,m_e^2)}{4m_e}\bar{u}(p')\sigma^{\mu\nu}(p+p')_\nu v(p) , \tag{10}$$

where

$$\mathrm{Re}[F_1(q^2,m_e^2)]=\frac{\alpha}{2\pi}\left[-2\ln\left[\frac{Q^2}{m_e^2}\right]\left[\frac{1}{n-4}+\frac{1}{2}\gamma_E-\frac{1}{2}\ln(4\pi)+\ln m_e\right]-\frac{1}{2}\ln^2\left[\frac{Q^2}{m_e^2}\right]+\frac{3}{2}\ln\left[\frac{Q^2}{m_e^2}\right]+O(1)\right] \tag{11}$$

and effects of F_2 are power suppressed. Also,

$$e^2\Pi_c(q^2)=-\frac{\alpha}{3\pi}\left[\ln\left[\frac{Q^2}{m_e^2}\right]+O(1)\right] . \tag{12}$$

The results from the one-loop vertex function and vacuum polarization modify the uncorrected result [Eq. (2)] in a simple way.

Combining the real-emission and virtual corrections,

$$\int_{(m_K-\Delta m)^2}^{m_K^2} dm_{\pi ee}^2 \frac{d\Gamma_{(3+4)}}{dm_{\pi ee}^2} \simeq \frac{1}{2m_K}\int\frac{d^3\mathbf{p}_\pi}{(2\pi)^3 2\epsilon_\pi}\int d^4q\,\theta[q^0-(\mathbf{p}_\pi^2)^{1/2}]\theta(q^2-q^2_{\mathrm{cut}})(2\pi)^4\delta^4(p_K-p_\pi-q)\frac{1}{8(2\pi)^6}$$
$$\times\int d^2\Omega_{\hat{\mathbf{R}}_1}\sum_{\mathrm{spins}}|\mathcal{M}_0(K\to\pi ee)|^2$$
$$\times\left\{1+\frac{\alpha}{\pi}\ln\left[\frac{Q^2}{m_e^2}\right]\left[\ln\left[\frac{m_K^2}{(Q+E_\pi)^2-(\hat{\mathbf{R}}_1\cdot\mathbf{P}_\pi)^2}\right]+2\ln\left[\frac{\Delta m}{m_e}\right]\right]\right.$$
$$\left.+\frac{\alpha}{\pi}\left[-\ln^2\left[\frac{Q^2}{m_e^2}\right]+\left[2\ln 2+\frac{19}{6}\right]\ln\left[\frac{q^2}{m_e^2}\right]\right]+O\left[\frac{\alpha}{\pi}\right]\right\} . \tag{13}$$

The dominant correction is the double logarithm $(\alpha/\pi)\ln^2(Q^2/m_e^2)$, which is numerically near 0.35 over the range $m_\pi^2<q^2<(m_K-m_\pi)^2$. Note that both the real-emission and virtual graphs contribute equally to it. That the dominant correction acts to suppress the tree result is due to the preference of the light leptons to radiate. These double logarithms are closely related to Sudakov double logarithms of the vertex function alone [11]. The Sudakov-like double logarithms in the vertex function with external fermions on shell are known to exponentiate when summed to all orders [12] in QED with a regulator photon mass in place. Assuming that the double logarithms here exponentiate as well when summed, the error in working to first order is not severe, e.g., $1-x-e^{-x}\simeq-0.05$ for $x=0.35$.

It is argued in the Appendix that the graphs of type Fig. 5 contribute presently incalculable terms proportional to $(\alpha/\pi)\ln m_e^2$ to Eq. (13). Therefore it is important to note that the terms proportional to $(\alpha/\pi)\ln m_e^2$ already appearing in Eq. (13) are not the complete set in the full result.

The recent results of [2] make possible a comparison of experiment and the results of this report, as shown in Fig. 6. The effects of an energy resolution of approximately 6 MeV have been folded into the predicted $m_{\pi ee}$ distribution. Improved correspondence between experiment and theoretical expectations is evident with the radiative corrections included.

To summarize the primary results, Eq. (8) describes the radiative tail to the $m_{\pi ee}$ distribution, and Eq. (13) contains the $O(\alpha)$ corrections to the contribution of the first bin of the $m_{\pi ee}$ distribution. Both contain the dominant logarithms. Equation (8) is subject to nonlogarithmic

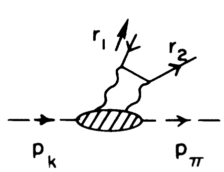

FIG. 5. Another class of virtual corrections, beyond that of Fig. 3.

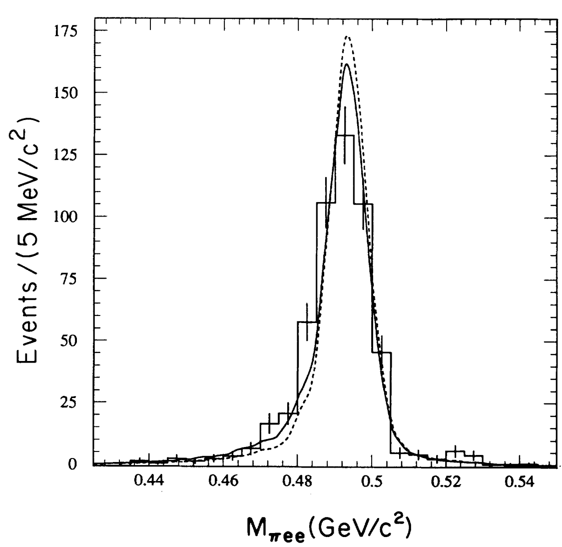

FIG. 6. Comparison of data (histogram) and Monte Carlo results from Ref. [2]. Monte Carlo results without (with) radiative corrections calculated here are given by the dashed (solid) curve.

corrections, while Eq. (13) is subject to additional single-logarithmic corrections, as described in the Appendix. Evaluation of the nonlogarithmic corrections would require both a more accurate calculation of the graphs considered here, as well as calculation of graphs in which the photon is radiated off of the K^+ or π^+. The arguments of the single logarithms cannot be fixed precisely without calculation of the nonlogarithmic terms for familiar reasons. Because $\ln(Q^2/m_e^2) \simeq 12$ over the appropriate range of Q^2, the corrections to both Eqs. (8) and (13) can be expected to be about 10% of the corrections as already given there.

ACKNOWLEDGMENTS

I thank C. Alliegro and M. Zeller, as well as W. Marciano, for very helpful conversations.

APPENDIX

The discussion of graphs of the form of Fig. 5 is somewhat heuristic because of the presence of apparently intractible hadronic complications. Contributions to the amplitude which are singular as $m_e^2 \to 0$, such as $\ln^2(m_e^2)$ or $\ln(m_e^2)$, arise from regions of soft or nearly lightlike loop momenta. Therefore, in analyzing such contributions, it is appropriate to organize the analysis according to the number of propagators which are singular in either region (or both).

The contributions most singular are those in which there is a single intermediate hadron, a π^+ or K^+. In either case one of the photons can be soft while the intermediate hadron is nearly on shell. The soft photon is emitted in the vertex, which does not change the variety of hadron. There are actually four graphs of this type; two are illustrated in Fig. 7. An approximate analysis of the contribution of Fig. 7(a) is as follows. In the most singular region, where the loop momentum l is soft, the l dependence of the propagator of the photon emitted in the K-to-π vertex is neglected. Dropping the l dependence of form factors as well, the contribution reduces to

$$\mathcal{M}_{7a} \simeq -ie^2 F(q^2) 4 r_2 \cdot p_K \, \bar{u}(r_2)\gamma_\lambda v(r_1) p_K^\lambda \, I(r_2, p_K) ,$$

where

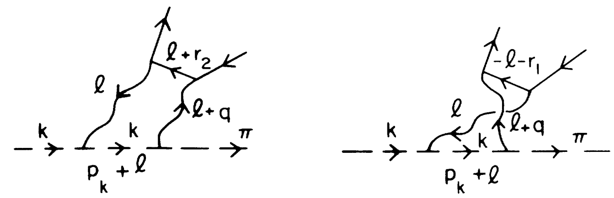

FIG. 7. Two examples of radiative corrections which fall into the class of Fig. 5.

$$I(r,p) = \int \frac{d^D l}{(2\pi)^D} \frac{1}{l^2 + 2l\cdot r + i\epsilon} \frac{1}{l^2 + i\epsilon} \times \frac{1}{l^2 + 2l\cdot p + i\epsilon} .$$

Keeping only terms singular as $r^2 = m_e^2 \to 0$,

$$I(r,p) \simeq -i \frac{\Gamma(3-D/2)}{(4\pi)^{D/2}} \times \left\{ \frac{1}{2r\cdot p} \left[\frac{1}{D-4} \ln\left[\frac{p^2}{m_e^2}\right] - \frac{1}{4}\ln^2(m_e^2) \right] \right\} ,$$

where the pole term, proportional to $1/(D-4)$, is a dimensionally regulated IR divergence. When this contribution is added to the corresponding contribution of Fig. 7(b), the IR divergences as well as the $\ln^2(m_e^2)$ terms cancel. It is of course necessary that the IR divergences cancel. The sum of the two graphs, approximated as before, in which the intermediate hadron is a π^+, is also free of IR divergences or singularities proportional to $\ln^2(m_e^2)$.

Integrals which are less singular for soft l can contain at most single logarithms of m_e^2. For example, the integral

$$\int \frac{d^D l}{(2\pi)^D} \frac{1}{l^2 + i\epsilon} \frac{1}{l^2 + 2l\cdot r + i\epsilon} J(p) ,$$

where $J(p) = l\cdot p/(l^2 + 2l\cdot p + i\epsilon)$ or $1/(l^2 + 2l\cdot p + M^2 + i\epsilon)$, contains a single logarithm of m_e^2. Such terms are very difficult to analyze because they depend on the details of form factors and/or the π-K Compton amplitude. Consequently, the graphs of type Fig. 5 contribute apparently incalculable terms proportional to $(\alpha/\pi)\ln m_e^2$ in Eq. (13).

[1] C. Campagnari *et al.*, Phys. Rev. Lett. **61**, 2062 (1988); A. M. Lee *et al.*, *ibid.* **64**, 165 (1990).
[2] C. Alliegro and M. Zeller (private communication).
[3] T. Kinoshita, Phys. Rev. Lett. **2**, 477 (1959); M. G. Smoes, Nucl. Phys. **B20**, 237 (1970); B. E. Lautrup and J. Smith, Phys. Rev. D **3**, 1122 (1971); A. Sirlin, *ibid.* **5**, 436 (1972).
[4] R. Gastmans and R. Meuldermans, Nucl. Phys. **B63**, 277 (1973).
[5] W. J. Marciano and A. Sirlin, Nucl. Phys. **B88**, 86 (1975).
[6] D. R. Yennie, S. C. Frautschi, and H. Suura, Ann. Phys. (N.Y.) **13**, 370 (1961).
[7] R. Gastmans, in *Quarks and Leptons,* edited by M. Levy *et al.* (Plenum, New York, 1980).
[8] G. Bonneau and F. Martin, Nucl. Phys. **B27**, 381 (1971).
[9] F. Berends, R. Gastmans, and K. J. F. Gaemers, Nucl. Phys. **B57**, 381 (1973).
[10] J. D. Bjorken and S. Drell, *Relativistic Quantum Mechanics* (McGraw-Hill, New York, 1964).
[11] V. V. Sudakov, Zh. Eksp. Teor. Fiz. **30**, 87 (1956) [Sov. Phys. JETP **3**, 65 (1956)].
[12] R. Jackiw, Ann. Phys. (N.Y.) **48**, 292 (1968); P. M. Fishbane and J. D. Sullivan, Phys. Rev. D **4**, 458 (1971); A. H. Mueller, *ibid.* **20**, 2037 (1979).